



SUB-ASSEMBLY TESTING OF LARGE BUCKLING-RESTRAINED UNBONDED BRACES

**Kohji NISHIMOTO¹, Yasuhiro NAKATA², Isao KIMURA³, Ian AIKEN⁴, Satoshi YAMADA⁵ and
Akira WADA⁶,**

SUMMARY

This paper describes results from sub-assembly testing of large buckling-restrained Unbonded BracesTM. A total of four Unbonded BracesTM, of two different yield forces and two different overall lengths, were tested. The specimens were tested in an inclined configuration to impose both axial and flexural deformations on the braces. The testing protocol was based upon that defined for *Qualifying Cyclic Tests of Buckling-Restrained Braces* contained in the *AISC/SEAOC Recommended Provisions for Buckling-Restrained Braced Frames*.

This study showed that the Unbonded BracesTM exhibited stable and repeatable hysteretic behavior at all levels of deformation.

1. INTRODUCTION

The number of Japanese structures utilizing the Unbonded Brace, manufactured by Nippon Steel Corporation, has grown steadily over the last 15 years, with the total number now greater than 300. To date, the Unbonded Brace has also been used in nearly 30 projects in the United States. The Unbonded Brace is composed of a steel core plate encased in a steel tube that is filled with mortar. The encasing mortar and steel tube together provide buckling stability for the brace, producing nearly symmetric post-yielding behavior in tension and compression. The transfer of axial load from the steel core to the surrounding mortar is limited by the presence of an “unbonding” material between the steel core plate and the mortar. Previous experimental testing in Japan, considered Unbonded Braces with yield forces up to

¹ Manager, Building Construction Div., Nippon Steel Corporation, Japan.

² Manager, Building Construction Div., Nippon Steel Corporation, Japan.

³ Manager, Building Construction Div., Nippon Steel Corporation, Japan.

⁴ Principal, Seismic Isolation Engineering, Inc., USA.

⁵ Associate Professor, Structural Engineering Research Center, Tokyo Institute of Technology, Japan.

⁶ Professor, Structural Engineering Research Center, Tokyo Institute of Technology, Japan.

3,900 kN. This paper describes results from recent testing conducted on inclined braces with yield forces up to 5,170 kN.

2. TEST SPECIMENS

2.1 Description of Test Specimens

The four Unbonded Braces tested were designated as either A-type or B-type, and all had yielding core plates with cruciform (+) cross-sections of Japanese Industrial Standard (JIS) SN400B steel. The two A-type braces had a core plate yielding area of 18,080 mm², corresponding to a yield force of 5,170 kN. The two B-type braces had an area of 11,648 mm² and a yielding force of 3,483 kN. Each pair consisted of a ‘short’ and a ‘long’ brace; the short braces (specimens A-1 and B-1) had an overall length of 4,221 mm and the long braces (specimens A-2 and B-2) had an overall length of 7,552 mm. Table 2.1 lists the brace dimensions and properties, while Figure 2.1 shows sketches of the four specimens.

The end connections for all four specimens utilized ASTM A490 1-1/8 in. (28.6 mm) diameter bolts with ‘semi-oversized’ (bolt diameter plus 1/8 in. (3.2 mm)) bolt holes. AISC standard size (STD) holes (bolt diameter plus 1/16 in. (1.6 mm))) were used in the connection splice plates. All connection faying surfaces were AISC Class A (SSPC SP3 finish).

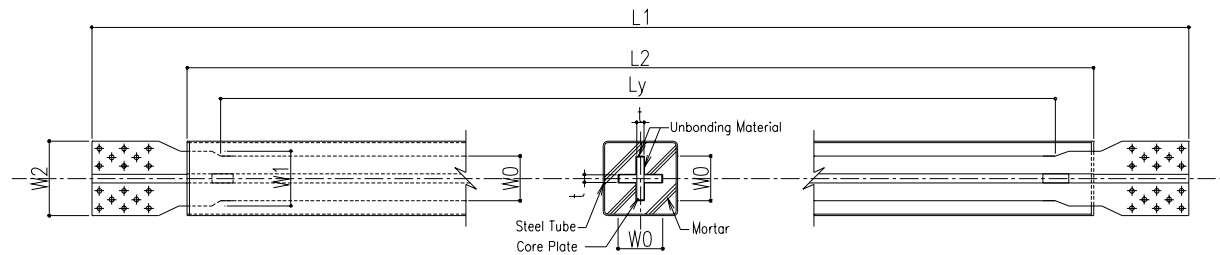


Figure 2.1 Configuration of Test Specimen

Table 2.1 Dimensions and Material Properties of Test Specimens

Brace Mark	Core PL Thk. T (mm)	Core PL Width W0 (mm)	W1 (mm)	W2 (mm)	Overall Length L1 (mm)	Tube Length L2 (mm)	Yielding Length Ly (mm)	Core PL Strength Fy (N/mm ²)	Core PL Area A (mm ²)	Yielding Force Py (kN)	SteelTube
A-1	40	246	396	550	4,221	3,197	2,747	286	18,080	5,170	BOX-450x450x12
A-2	40	246	396	550	7,552	6,498	6,018	286	18,080	5,170	BOX-450x450x12
B-1	28	222	300	432	4,221	3,237	2,907	299	11,648	3,483	BOX-350x350x9
B-2	28	222	300	432	7,552	6,538	6,178	299	11,648	3,483	BOX-350x350x9

3. TEST SETUP AND LOADING PROTOCOL

3.1 Test Setup

The test setup consisted of a pin-ended propped column supported by a single Unbonded Brace as shown in Figures 3.1 and 3.2. The free end of the column was loaded horizontally by three hydraulic actuators

that reacted against a vertical strong-wall. The base of the test setup consisted of two 10.5 m long reaction beams fixed to the laboratory strong-floor. Two of the actuators had capacities of 2,000 kN and the third 3,000 kN, giving a total horizontal force of 7,000 kN. The displacement capacity of all three actuators was ± 250 mm.

The sub-assembly test configuration represented the geometry and loading conditions for braces in a full-size single bay of a building, with a bay width of approximately 8,900 mm and a story height of 4,500 mm. The short brace configuration was intended to represent one brace of a chevron (inverted-v) configuration (or a short-bay single-diagonal brace), while the long brace configuration represented a long-bay single-diagonal brace.



Figure 3.1 Photo of Test Setup for B-2 Brace

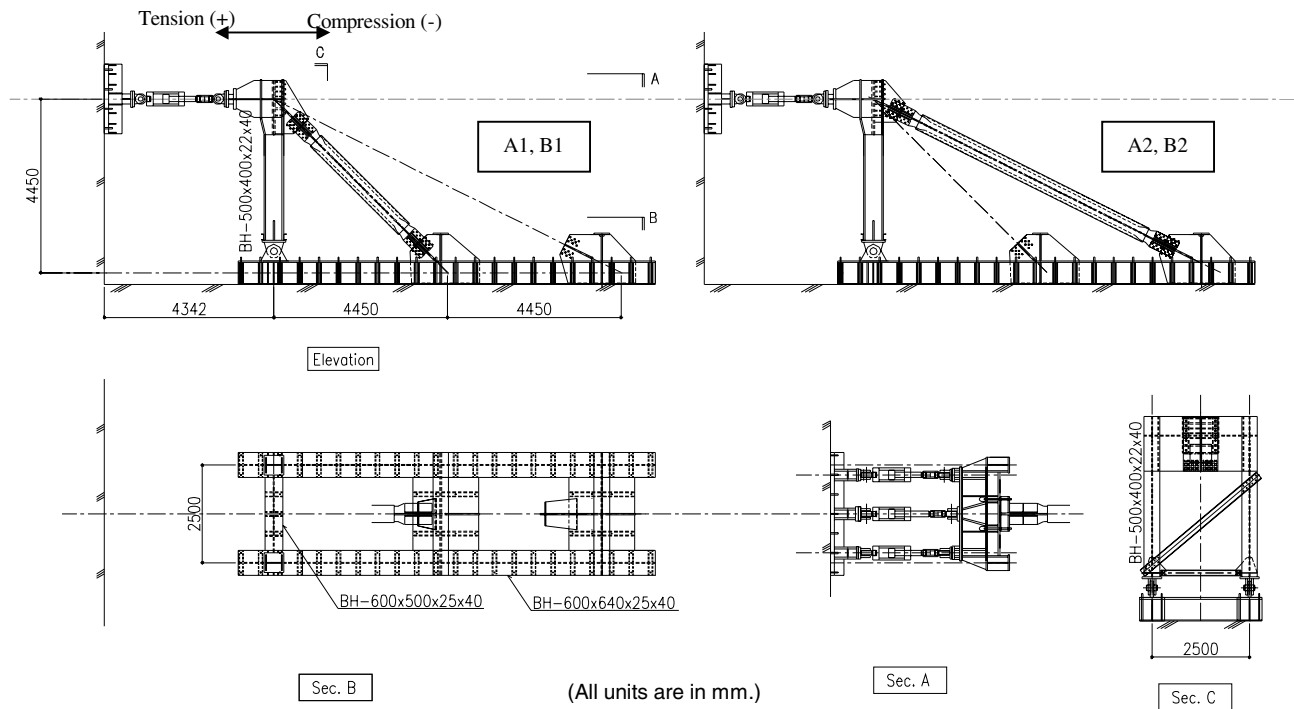


Figure 3.2 Plan and Elevation Views of Test Setups

3.2 Instrumentation

Test force and displacement quantities of interest were recorded via a digital data acquisition system. The displacement instrumentation on the test frame and brace specimen consisted of 30 wire potentiometers and direct current displacement transducers. A total 12 strain gauges (in three sets of four) oriented to measure axial strain were included on the outside of the confining tube, at the brace mid-length point and near each end. Force transducers, in-line with the actuators, measured the horizontal forces applied to the test assembly.

3.3 Loading Protocol

The four specimens were subjected to a loading program consisting of increasing amplitude elastic and post-yield cycles of displacement based on the recommendations for *Qualifying Cyclic Tests of Buckling-Restrained Braces* contained in the *AISC/SEAOC Recommended Provisions for Buckling-Restrained Braced Frames*. The loading program was designed to impose pre- and post-yield, fully reversed, displacement corresponding to: the brace yield displacement, 0.5, 1.0 and 1.5 times the maximum expected brace deformation at the design story drift, as well as the brace deformation corresponding to 2.5% story drift. For the purposes of the testing program, the design story drift was assumed to be 1.5%. Additional loading cycles corresponding to 3.0% story drift were imposed on the B-type braces in order to study the fatigue characteristics of the braces.

The Brace Loading History is shown in Figure 3.3, with the specific details for the four specimens given in Table 3.1; Δ_{by} corresponds to the brace axial deformation at first significant yield and Δ_{bm} corresponds to the brace axial deformation at the design story drift.

As a result of the way that the displacement loading history was applied to the test sub-assembly during the tests, the actual story drifts imposed were larger than the test target values. Table 3.1 lists the Target Story Drift for each test amplitude increment, as well as the Actual Story Drift that was imposed for each test specimen. It can be seen from the table that the largest brace deformations for specimens A-1 and A-2 corresponded to story drifts of approximately 3%, and for specimens B-1 and B-2 approximately 3.6%.

Table 3.1 Brace Loading History

Brace mark	Loading No.	1	2	3	4	5	6
	SEAO	Δ_{by}	0.5 Δ_{bm}	1.0 Δ_{bm}	1.5 Δ_{bm}	1.67 Δ_{bm}	2.0 Δ_{bm}
	Target Story Drift (%)		+/-0.75	+/-1.5	+/-2.25	+/-2.5	+/-3.0
	Nos. of Cycle	6	4	4	2	2	*
A-1	Horizontal Disp. (mm)	5.41	33.4	66.8	100.1	111.3	
	Actual Story Drift (%)		1.07	1.97	2.95	3.23	
	Axial Deformation (mm)	3.82	23.6	47.2	70.8	78.7	
	Axial Strain (%)	0.14	0.86	1.72	2.58	2.86	
A-2	Horizontal Disp. (mm)	9.37	33.4	66.8	100.1	111.3	
	Actual Story Drift (%)		0.91	1.80	2.70	3.00	
	Axial Deformation (mm)	8.38	29.9	59.7	89.6	99.5	
	Axial Strain (%)	0.14	0.5	0.99	1.49	1.65	
B-1	Horizontal Disp. (mm)	5.98	33.4	66.8	100.1	111.3	133.5
	Actual Story Drift (%)		0.90	1.79	2.69	2.96	3.63
	Axial Deformation (mm)	4.2	23.6	47.2	70.8	78.7	94.4
	Axial Strain (%)	0.15	0.81	1.62	2.44	2.71	3.25
B-2	Horizontal Disp. (mm)	10.1	33.4	66.8	100.1	111.3	133.5
	Actual Story Drift (%)		0.89	1.80	2.68	2.98	3.58
	Axial Deformation (mm)	8.99	29.9	59.7	89.6	99.5	119.4
	Axial Strain (%)	0.15	0.48	0.97	1.45	1.61	1.93

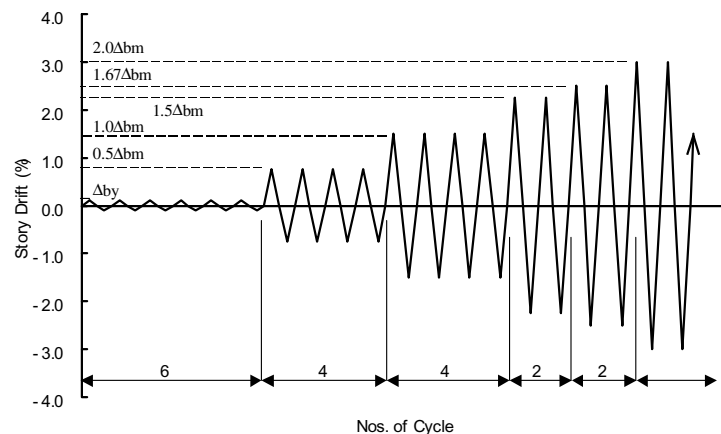


Figure 3.3 Brace Loading History

4. TEST RESULTS

4.1 Force-Deformation Behavior

Figure 4.1 plots the brace axial stress vs. axial strain for each of the four specimens. The axial stress was calculated using the brace axial force (resolved component of applied horizontal force), divided by the initial core plate area, and the axial strain was calculated using the measured axial deformation over the yield length of the core plate.

It is seen from Figure 4.1 that all four specimens exhibited stable, repeatable hysteretic behavior with positive incremental stiffness for all cycles of loading.

As shown in Table 4.1, the ratios of brace maximum compression force to maximum tension force range from 1.00 to 1.10, and thus satisfy the requirement of section ABRB.10 of the *AISC/SEAOC Recommended Provisions*, which states that this ratio must not to exceed 1.3. The reasons for the maximum compression force being larger than the maximum tension force are: 1) the variation of the core plate area due to Poisson's Ratio and 2) contact forces that develop between the core plate and encasing mortar in compression.

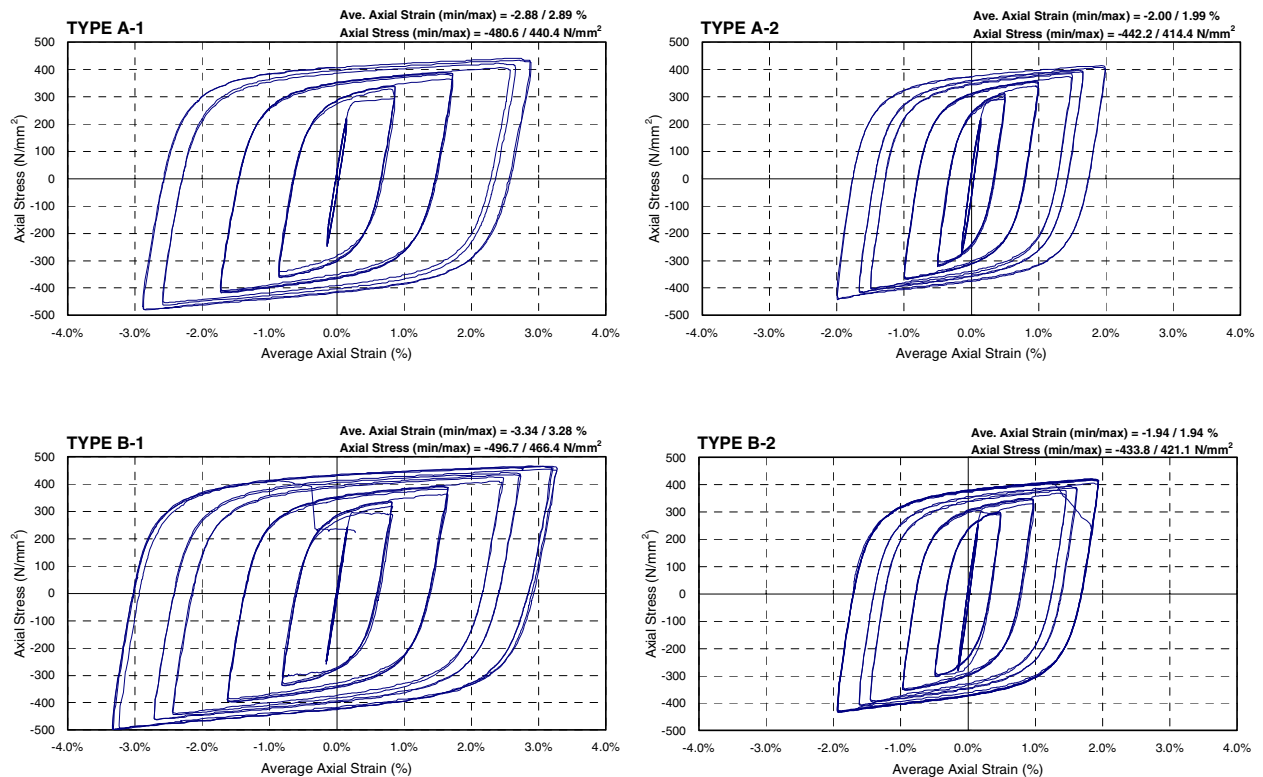


Figure 4.1 Axial Stress vs. Average Axial Strain

Table 4.1 Maximum Tension and Compression Forces

Brace Mark	LoadingNo.	2	3	4	5	6
		0.5 Δ bm	1.0 Δ bm	1.5 Δ bm	1.67 Δ bm	2.0 Δ bm
A-1	Tension, Pt (kN)	6,131	7,043	7,640	7,963	
	Compression, Pc (kN)	6,541	7,560	8,369	8,688	
	Pc/Pt	1.07	1.07	1.10	1.09	
A-2	Tension, Pt (kN)	5,642	6,429	6,952	7,176	
	Compression, Pc (kN)	5,809	6,642	7,307	7,532	
	Pc/Pt	1.03	1.03	1.05	1.05	
B-1	Tension, Pt (kN)	3,947	4,566	4,969	5,152	5,433
	Compression, Pc (kN)	3,936	4,636	5,170	5,387	5,809
	Pc/Pt	1.00	1.02	1.04	1.05	1.07
B-2	Tension, Pt (kN)	3,509	4,065	4,424	4,581	4,905
	Compression, Pc (kN)	3,526	4,109	4,613	4,751	5,053
	Pc/Pt	1.00	1.01	1.04	1.04	1.03

4.2 Brace Rotational Deformation

In order to characterize the bending deformations that occurred in the brace test specimens, the following rotational deformations (shown in Figure 4.2) were measured: 1) the column rotation, θ_f , 2) the brace axis rotations, θ_{br-u} and θ_{br-b} , 3) the brace end rotations, θ_{e-u} and θ_{e-b} and 4) the flexural rotations of the steel tube, θ_{p-u} and θ_{p-b} . Figure 4.3 summarizes the rotational deformations as a function of story drift for each specimen. It is seen that for the longer braces, specimens A-2 and B-2, the upper end of the brace (connected to the propped column) experienced rotations three to five times greater than at the lower end (connected to the floor).

On the other hand, for the shorter braces (A-1 and B-1), the difference in rotational deformation between the upper and lower brace ends is less significant. Figure 4.3 also indicates that the flexural rotations at the ends of the steel tube, θ_{p-u} and θ_{p-b} , are similar.

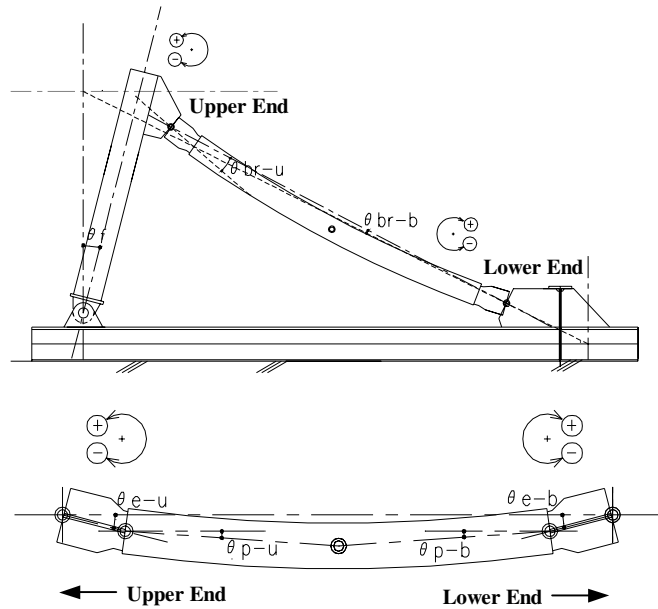


Figure 4.2 Definition of Rotational Deformation

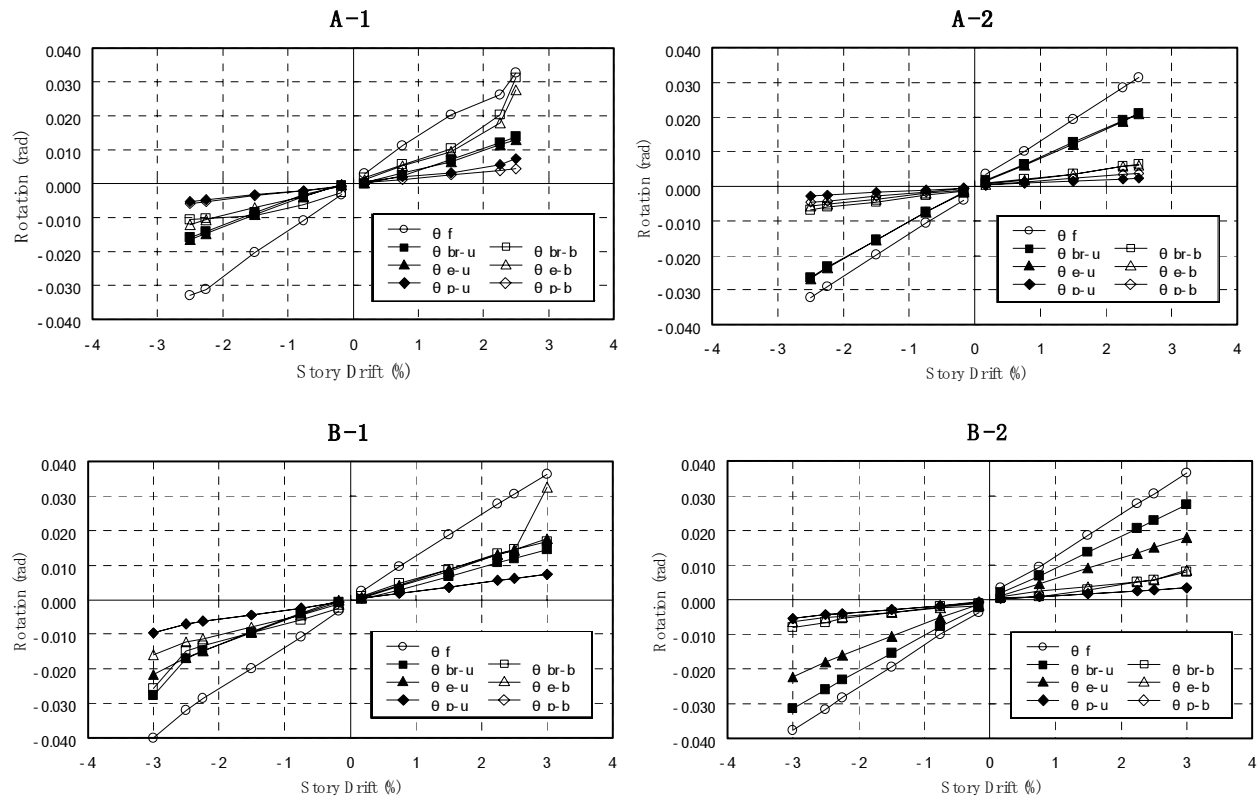


Figure 4.3 Brace Rotational Deformations

4.3 Fatigue Properties

As mentioned previously, specimens B-1 and B-2 were subjected to additional low-cycle fatigue testing at a story drift of approximately 3.6%. Brace B-1 completed three cycles before a loss of strength was observed, while brace B-2 maintained its strength for eight cycles before failing in tension.

Table 4.2 summarizes the cumulative plastic strain ($\Sigma\epsilon_p$) for each specimen. The total cumulative plastic strain for all tests conducted on specimen B-1 was 121%, and for specimen B-2 the total cumulative plastic strain was 89.8%. These values of cumulative plastic strain are comparable with results obtained in other sub-assembly testing programs (Hasegawa et al. 1999), and somewhat less than those for braces subjected to uni-axial only loading (Black et al. 2004; Clark et al. 2000; Maeda et al. 1999).

Table 4.2 Brace Displacements and Ductilities

Brace Mark	Loading No.		1	2	3	4	5	6
			Δ_{by}	0.5 Δ_{bm}	1.0 Δ_{bm}	1.5 Δ_{bm}	1.67 Δ_{bm}	2.0 Δ_{bm}
	Story Drift (%)		0.75	1.5	2.25	2.5	3.0	
	Nos. of Cycle		6	4	4	2	2	*
A-1	Brace Displacement	δ_{br} (mm)	8.30	47.9	95.8	145.2	158.7	
	Brace Strain	ϵ_{br} (%)	0.30	1.74	3.49	5.28	5.78	
		ϵ_p (%)		1.41	3.15	4.95	5.44	
		$\Sigma \epsilon_p$ (%)		11.3	36.5	56.1	77.9	
A-2	Brace Displacement	δ_{br} (mm)	17.7	61	120.6	181	200.7	
	Brace Strain	ϵ_{br} (%)	0.29	1.01	2.00	3.01	3.34	
		ϵ_p (%)		0.68	1.67	2.67	3	
		$\Sigma \epsilon_p$ (%)		5.40	18.8	29.5	41.5	
B-1	Brace Displacement	δ_{br} (mm)	9.10	47.6	95.5	142.9	158.3	190
	Brace Strain	ϵ_{br} (%)	0.31	1.64	3.28	4.92	5.45	6.54
		ϵ_p (%)		1.26	2.9	4.54	5.07	6.16
		$\Sigma \epsilon_p$ (%)		10.1	33.3	51.4	71.7	121
B-2	Brace Displacement	δ_{br} (mm)	18.7	61.1	120.7	181.1	201.1	240.6
	Brace Strain	ϵ_{br} (%)	0.30	0.99	1.95	2.93	3.26	3.89
		ϵ_p (%)		0.64	1.61	2.58	2.91	3.55
		$\Sigma \epsilon_p$ (%)		5.20	18.1	28.4	40.1	89.8

5. CONCLUSIONS

This paper has summarized results from the testing of large Unbonded Braces in a subassembly configuration. The following conclusions are drawn:

- 1) The four test specimens satisfied all the test acceptance criteria defined in the *AISC/SEAOC Recommended Provisions for Buckling-Restrained Braced Frames*, and specimens B-1 and B-2 were shown to have substantial overall fatigue resistance for deformations corresponding to story drift ratios up to approximately 3.6%.
- 2) It was observed experimentally that the rotational deformation of the end of a brace depends on its inclination, and that the rotational deformation was greater at the brace end connected to the propped column than at the lower end. This result was particularly true for the longer braces (with smaller inclination angle).

ACKNOWLEDGEMENTS

The contributions made by Mr. Eric Ko of Arup San Francisco and Mr. Walterio Lopez of Rutherford & Chekene to the testing program are acknowledged.

REFERENCES

1. Black, C.J., Makris, N., Aiken, I.D. (2004). "Component Testing, Seismic Evaluation and Characterization of buckling-restrained braces," *J. of Structural Engineering*, American Society of Civil Engineers, Vol.130, No.6.
2. Clark, P.W., Aiken, I.D., Kasai K., Kimura, I. (2000). "Large-Scale Testing of Steel Unbonded Braces for Energy Dissipation," *Proceedings, Structures Congress 2000*, ASCE/SEI, Philadelphia, Pennsylvania.
3. Maeda, Y., Nakata, Y., Iwata, M., Wada, A. (1998). "Fatigue Properties of Axial-Yield Type Hysteresis Dampers," *Journal of Structural and Construction Engineering*, Architectural Institute of Japan, No.503 (in Japanese).
4. Maeda, Y., Nakamura, H., Takeuchi, T., Nakata, Y., Iwata, M., Wada, A. (1999). "Fatigue Properties of Practical-Scale Unbonded Braces (Part 1 and Part 2)," *Annual Meeting of the Architectural Institute of Japan* (in Japanese).
5. Hasegawa, H., Takeuchi, T., Nakata, Y., Iwata, M., Yamada, S., Akiyama, H. (1999). "Experimental Study on Dynamic Behavior of Unbonded Braces," *AII J. Technol. Des. No.9* (in Japanese).
6. Saeki, E., Iwamatu K., Wada A. (1996). "Analytical Study by Finite Element Method and Comparison with Experiment Results Concerning Buckling-Restrained Unbonded Braces," *Journal of Structural and Construction Engineering*, Architectural Institute of Japan, No.484 (in Japanese).
7. Saeki, E., Maeda, Y., Iwamatu K., Wada A. (1996). "Analytical Study on Unbonded Braces fixed in a Frame," *Journal of Structural and Construction Engineering*, Architectural Institute of Japan, No.489 (in Japanese).
8. AISC/SEAOC (2001). "Recommended Provisions for Buckling-Restrained Braced Frames," American Institute of Steel Construction/Structural Engineers Association of California Task Group, October.
9. AISC (2001). "Manual of Steel Construction Load and Resistance Factor Design Third Edition," American Institute of Steel Construction.